

## Recent widening of the tropical belt from global tropopause statistics: Sensitivities

Thomas Birner<sup>1</sup>

Received 22 June 2010; revised 25 August 2010; accepted 24 September 2010; published 3 December 2010.

[1] Several recent studies have shown evidence for a widening of the tropical belt over the past few decades. One line of evidence uses statistics of the tropopause height to distinguish between tropics and extratropics and defines tropical edge latitudes as those latitudes at which the number of days per year with tropopause heights greater than 15 km exceeds a certain threshold (typically 200 days/yr). This definition involves two somewhat arbitrary thresholds. Here the sensitivity of the resulting widening trend of the tropical belt to these thresholds is investigated using four different reanalysis data sets. Widening trends are found to be particularly sensitive to changes in the tropopause height threshold. Ways to objectively determine appropriate thresholds to define tropical edge latitudes based on tropopause statistics are presented. Trend estimates for the width of the tropical belt from different reanalysis data sets are found to be mostly inconsistent with each other despite consistent seasonal and interannual variations.

**Citation:** Birner, T. (2010), Recent widening of the tropical belt from global tropopause statistics: Sensitivities, *J. Geophys. Res.*, 115, D23109, doi:10.1029/2010JD014664.

### 1. Introduction

[2] Several recent studies have shown evidence for a widening of the tropical belt over the past few decades (see, e.g., the overview by *Seidel et al.* [2008]). *Lu et al.* [2009] have attributed this widening trend to anthropogenic climate change, in particular to the direct radiative forcing associated with changes in greenhouse gases and stratospheric ozone depletion. Independent of its cause, a widening of the tropical belt has important consequences for global climate, for example, a poleward shift of the subtropical jet streams with implications for midlatitude storm tracks, as well as a poleward shift of the subtropical dry zones associated with a greater potential for midlatitude droughts [e.g., *Hu and Fu*, 2007].

[3] Existing measures of the width of the tropical belt are based on a threshold in total column ozone concentrations [*Hudson et al.*, 2006], the zero crossing of the mean meridional mass stream function [*Frierson et al.*, 2007; *Hu and Fu*, 2007; *Lu et al.*, 2007; *Johanson and Fu*, 2009], a threshold in outgoing longwave radiation [*Hu and Fu*, 2007; *Johanson and Fu*, 2009], and the frequency of high tropopause levels [*Seidel and Randel*, 2007] (hereafter SR07). Here the focus is on the latter measure of the width of the tropical belt based on specific characteristics of the frequency distribution of tropopause height as introduced by SR07 and recently used by *Lu et al.* [2009].

[4] SR07 employ the fact that frequency distributions of tropopause height in the subtropics show a bimodal structure with one mode corresponding to tropical tropopause heights and one mode corresponding to extratropical tropopause heights. They then classify a given location as tropical if the number of days per year with a tropopause higher than 15 km exceeds a certain threshold (typically 200 d/yr; SR07 also consider 100 and 300 d/yr). Obviously this definition involves two somewhat arbitrary thresholds: one for a minimum tropical tropopause height (15 km) and one for the frequency of occurrence (e.g., 200 d/365 days  $\approx$  0.55). In the present study the sensitivity of the resulting widening trend to changes in these thresholds is investigated. It is shown that the reanalysis tropopause data as used by SR07 (and by *Lu et al.* [2009]) yields strong sensitivity of the widening trend to changes in the thresholds (note that this does not necessarily carry over to the trends based on radiosonde data in SR07). Moreover, the reanalysis tropopause data as used by these authors is found to be problematic for the evaluation of long-term trends.

[5] Possible objective criteria to define the width of the tropical belt based on hemispheric statistics of tropopause height are then derived and applied to four reanalysis data sets. One approach employs the idea that a tropopause height threshold above which tropopause height is considered to be tropical should be defined such that the resulting estimate of the width of the tropical belt shows small sensitivity to (reasonable) changes in this threshold. Another approach relates the tropopause height threshold to statistics of the inner tropical tropopause height. Both approaches allow the tropopause height threshold to be a function of time, hemisphere, and data set used. Widening trends based on these objective criteria will be shown to be mostly

<sup>1</sup>Department of Atmospheric Science, Colorado State University, Fort Collins, Colorado, USA.

inconsistent between different reanalyses. It is therefore concluded that tropopause statistics based on current reanalysis data sets may not serve as an appropriate way to quantify long-term changes in the width of the tropical belt.

[6] The paper is structured as follows. Section 2 shortly describes the data sets used and discusses the tropopause definition. Section 3 presents the sensitivity analysis of the SR07 definition of tropical width to changes in the thresholds involved. Section 4 presents possible ways to objectively define the width of the tropical belt based on global tropopause statistics and section 5 presents the resulting widening trends. Section 6 summarizes the results and concludes the paper.

## 2. Data and Tropopause Definition

[7] Four sets of reanalysis data are employed in the present study: NCEP/NCAR (hereafter referred to as NCEP) [Kalnay *et al.*, 1996; Kistler *et al.*, 2001], NCEP/DOE (hereafter referred to as NCEP2) [Kanamitsu *et al.*, 2002], ERA40 [Uppala *et al.*, 2005], and JRA25 [Onogi *et al.*, 2007]. All of these data sets are used on their native model levels on a regular  $2.5^\circ$  grid. It is believed to be important to use model level data since the derived tropopause product is sensitive to the underlying resolution of the temperature profiles, in particular for coarse resolution global models. Vertical resolution near the subtropical tropopause ( $\sim 200$  hPa) ranges from  $\sim 1.5$  km (NCEP, NCEP2) to  $\sim 1.1$  km (JRA25) to  $\sim 0.9$  km (ERA40). The degree of representation of the stratosphere is also noteworthy: NCEP and NCEP2 have only 6 levels above 100 hPa, JRA25 has 13 levels above 100 hPa, whereas ERA40 has 25 levels above 100 hPa. Given the coarse vertical resolution even in the underlying models it is crucial to use model level data as opposed to standard pressure levels. The time period used is 1979–2009, except for ERA40 for which full years are only available until 2001.

[8] Six-hourly tropopause data are obtained for each reanalysis data set based on the WMO definition of the thermal tropopause [World Meteorological Organization, 1957]: the thermal tropopause corresponds to the lowest level at which the lapse rate falls below 2 K/km, provided the average lapse rate between this level and all higher levels within 2 km remains below 2 K/km. This tropopause definition consists of two criteria: (1) a stratification threshold above which air is classified stratospheric and (2) a thickness criterion which prevents thin stable layers from being identified as stratospheric. This definition is implemented as follows (except for the implementation of the thickness criterion the algorithm below is identical to that of Reichler *et al.* [2003], who describe the application of the thermal tropopause definition to coarse-resolution model data).

[9] The thermal tropopause definition requires lapse rate profiles  $\Gamma \equiv -\partial_z T$  (where  $T$  is temperature) which have to be obtained first given all models considered here work in pressure-like coordinates. A complicating factor is that model levels are not evenly spaced in pressure ( $p$ ); however, they are more evenly spaced in  $\sigma = (p/p_0)^\kappa$ , where  $\kappa = R/c_p \approx 2/7$  ( $R$  is the specific gas constant and  $c_p$  is the heat capacity at constant pressure) and  $p_0 = 1000$  hPa. The altitude spacing  $\Delta z_{k+1/2}$  between two consecutive model levels

$k$  and  $k + 1$  with the convention  $z_k < z_{k+1}$  is therefore obtained as

$$\Delta z_{k+1/2} = -RT_{k+1/2} \frac{\sigma_{k+1} - \sigma_k}{g\kappa\sigma_{k+1/2}}.$$

Using the resulting lapse rate on half levels ( $\Gamma_{k+1/2}$ ), the lowest level above 500 hPa is obtained for which  $\Gamma_{k+1/2} < 2$  K/km and  $\Gamma_{k-1/2} > 2$  K/km. Next a preliminary tropopause level is obtained by interpolating  $\sigma$  between levels  $k - 1/2$  and  $k + 1/2$  onto  $\Gamma = 2$  K/km. This tropopause level is only accepted if the thickness criterion is fulfilled, i.e., if all average lapse rates between tropopause level and all higher levels within 2 km are less than 2 K/km. It is important to note that this is more restrictive than simply requiring the (single) average lapse rate over all levels within 2 km above tropopause level to be less than 2 K/km (Reichler *et al.* [2003] seem to apply this latter less restrictive criterion). Tests with different ways to implement the thickness criterion revealed little sensitivity for almost all latitudes (given the coarse vertical resolution of current global models this does not seem surprising). However, subtropical latitudes, the key region for studies on the width of the tropical belt, constitute an exception with strong sensitivity to the way the thickness criterion is implemented. Again, this does not seem surprising given the complicated stratification structure and associated double tropopause structure that is frequently observed in the subtropics [e.g., Randel *et al.*, 2007; Añel *et al.*, 2008]. An analysis of the frequency with which the thickness criterion led to a modified tropopause level showed that this frequency maximizes in the subtropics (near  $30^\circ$  latitude) for all data sets, with climatological annual mean maximum frequencies between 6 and 13%. In the subtropics where double-tropopause structures are most prominent the thickness criterion therefore prevents the acceptance of the lower one of these tropopauses about 10% of the time.

[10] Tropopause pressure  $p_{\text{TP}}$  is obtained from the definition of  $\sigma$ . Tropopause geopotential height  $z_{\text{TP}}$  follows by vertically integrating the hydrostatic relation:  $z_{\text{TP}} = z_0 - R/g \int_{p_{\text{sfc}}}^{p_{\text{TP}}} T d \ln p$  (where  $z_0$  is the height of the orography,  $g$  is the acceleration due to gravity, and  $p_{\text{sfc}}$  is surface pressure). All tropopause heights used in this study refer to this geopotential height at tropopause level, unless stated otherwise. Note that log-pressure height  $\tilde{z}$  can be considered an approximation of geopotential height (taking  $T = T_m = \text{const.}$ ,  $z_0 = 0$ , and  $p_{\text{sfc}} = p_0 = 1000$  hPa), such that  $\tilde{z} = H \ln(p_0/p)$ .  $H \equiv RT_m/g$  is the scale height (typically  $H = 7$  km, corresponding to  $T_m \approx 240$  K). That is, log-pressure height has a one-to-one relationship with pressure, while geopotential height also depends on the temperature structure (and to a lesser degree on surface elevation and pressure).

[11] A tropopause product (pressure and temperature) for NCEP is also provided as part of their data set. However, this tropopause is obtained by applying only part of the WMO definition; the thickness criterion is not applied (W. Ebisuzaki, personal communication, 2010). More importantly, this tropopause is obtained by using coarse-grained three-point centered differences to compute lapse rate profiles (i.e., including both nearest neighbors of a given level). This acts to smooth profiles in addition to the coarse vertical resolution of the model. The smoothing due

to the use of coarse-grained centered differences and the neglect of the thickness criterion lead to discrepancies with tropopause estimates based on the WMO definition. Special care should therefore be applied to the operational NCEP tropopause product. The use of this product to study long-term changes should be avoided, especially in the subtropics where the sensitivity to the way the tropopause is implemented is largest. SR07 and *Lu et al.* [2009] rely on this operational NCEP tropopause product, it is therefore included here for comparison and labeled NCEP\*.

### 3. Sensitivity of the SR07 Results to Changes in the Thresholds Used

[12] SR07 define edge latitudes of the tropics as those latitudes (in the Southern and Northern Hemisphere) at which the number of days per year with tropopause heights above 15 km equals a certain threshold (SR07 show results for 100, 200, and 300 days; *Lu et al.* [2009] use the 200 days threshold). This definition allows the tropical edge latitudes to be a function of longitude, here only the zonal means of these edge latitudes are considered. Note, the 200 days threshold corresponds to a frequency of occurrence of 55%, which is very close to one half. This definition for the width of the tropics involves two somewhat arbitrary thresholds. These thresholds will be referred to as tropopause height threshold ( $z_{TP}^*$ ) and frequency threshold.

[13] It is important to note that the tropopause height threshold is applied somewhat ambiguously by SR07: for the radiosonde data the tropopause height threshold of 15 km refers to geopotential height, whereas it refers to a log-pressure height using a scale height of 7 km in the case of the NCEP\* model data (B. Randel, personal communication, 2010). Thus the NCEP\* tropopause height threshold from SR07 really refers to a pressure threshold of about 117 hPa (in fact, *Lu et al.* [2009] use a pressure threshold of 120 hPa). Log-pressure height and geopotential height are generally not equal (see section 2); using a scale height of 7 km, they differ by about 500 m in the altitude range of interest (near the subtropical tropopause). That is, a log-pressure threshold of 15 km corresponds to a geopotential height threshold of about 15.5 km (likewise the geopotential height threshold of 15 km used for the radiosonde data from SR07 corresponds to a log-pressure threshold of about 14.5 km).

[14] Figure 1 shows tropical belt widening trends over the period 1979–2005 (as in work by SR07) as a function of the frequency threshold and the tropopause height threshold based on the statistics of different estimates of tropopause height from NCEP data: operational NCEP (NCEP\*) tropopause pressure converted into log-pressure height using a scale height of 7 km as in work by SR07 (Figure 1, left), tropopause (geopotential) height based on NCEP\* (Figure 1, middle), and tropopause height based on NCEP temperature profiles computed using the WMO definition as described in section 2 (Figure 1, right). Trends, where statistically significant (based on  $2\sigma$  uncertainties), are exclusively positive (corresponding to widening) and lie in the range of  $\sim 1$ – $2^\circ$ /decade for most of the considered threshold combinations.

[15] However, substantial sensitivity of the widening trend to changes in the thresholds exists in particular for

the operational NCEP tropopause data, especially to changes in the tropopause height threshold. Sensitivity to the frequency threshold is apparently not as strong as long as this threshold stays in the neighborhood of 200 days. For reference, the particular trends obtained for the thresholds used in SR07 (15 km and either 100, 200, or 300 d/yr) are: 1.7, 1.8, and  $2.8^\circ$ /decade. Trends for the 100 and 200 d/yr frequency thresholds agree exactly with the ones reported by SR07, whereas the trend for the 300 d/yr frequency threshold deviates slightly (but is well within the range of uncertainty).

[16] Using tropopause height instead of log-pressure height reduces the sensitivity of the trend to changes in the thresholds somewhat, in particular for tropopause height thresholds above 15 km. This result may seem surprising given essentially the same tropopause data is used as in Figure 1 (left). However, as discussed above, log-pressure height and geopotential height differ by about 500 m in the altitude range of interest; indeed, when shifted toward higher tropopause height thresholds by about 500 m, Figure 1 (left) agrees well with Figure 1 (middle). It should also be noted that tropopause pressure tends to more heavily cluster around model levels than tropopause height. This is because model (sigma) levels are much more directly related to a given pressure than to a given geopotential height.

[17] Using tropopause heights computed offline from the NCEP temperature data using the correct WMO definition (Figure 1, right) results in much reduced sensitivity of the widening trend to changes in the thresholds, in particular for tropopause height thresholds within 14–15 km and frequency thresholds around 200 d/yr. For reference, for the SR07 thresholds of 15 km and 200 d/yr a trend of  $0.7 \pm 0.4^\circ$ /decade is obtained in this case (which happens to be consistent with the 1958–1999 trend reported by *Lu et al.* [2009] based on NCEP\* tropopause pressure data, using a threshold of 120 hPa).

### 4. Toward an Objective Definition of the Width of the Tropical Belt

[18] In this section a method is described that leaves the tropopause height threshold as the only free parameter of the problem. Then, ways to objectively determine a tropopause height threshold are discussed.

#### 4.1. Width of the Tropical Belt as a Function of the Tropopause Height Threshold

[19] For a given tropopause height threshold  $z_{TP}^*$  the tropical edge latitude in each hemisphere is obtained by first calculating the hemispheric area  $A_{S,N}$  covered by tropical tropopause heights ( $z_{TP} > z_{TP}^*$ ) normalized by the total area of one hemisphere. That is, the area-weighted hemispheric integral of the frequency of occurrence of tropical tropopause heights is calculated. For example, if all tropopause heights over the whole hemisphere were tropical, then  $A_{S,N} = 1$ . If all tropopause heights equatorward of  $30^\circ$  were tropical, then  $A_{S,N} = 1/2$ . The tropical edge latitudes  $\varphi_{S,N}$  corresponding to this normalized hemispheric area are then defined through

$$A_{S,N} = \sin \varphi_{S,N}.$$

This definition shares the general flavor of area-based coordinates such as equivalent latitude [e.g., *Butchart and*

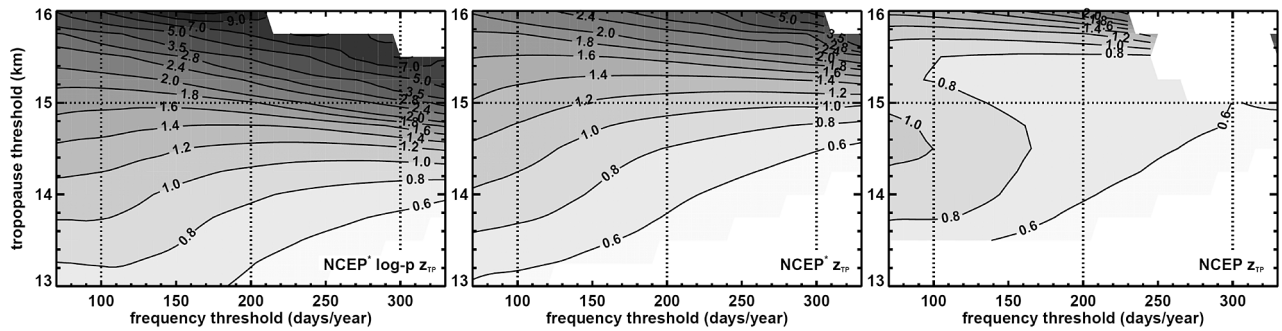


**Figure 1.** Trends in the width of the tropical belt ( $^{\circ}$ /decade) for the period 1979–2005 as a function of the number of days per year (frequency threshold, abscissa) the tropopause height is above a certain threshold (tropopause height threshold, ordinate). (left) Log-pressure tropopause height (scale height 7 km) based on tropopause product provided by NCEP (named NCEP\*) as used by SR07. (middle) tropopause geopotential height based on NCEP\*. (right) tropopause geopotential height obtained offline from NCEP model level temperature data by applying the WMO definition. Only significant trends (based on  $2\sigma$  uncertainties) are shown.

Remsburg, 1985]. A basic associated property is that  $\varphi_{S,N}$  is a monotonic function of  $z_{TP}^t$ .  $A_{S,N}(z_{TP} > z_{TP}^t)$  defined as described above corresponds uniquely to the area-weighted hemispheric cumulative tropopause height frequency ( $f_c^{S,N}$ ) at  $z_{TP}^t$  through

$$A_{S,N}(z_{TP} > z_{TP}^t) = 1 - f_c^{S,N}(z_{TP} = z_{TP}^t).$$

[20] Figure 2 shows the annual mean frequency of occurrence of  $z_{TP} > 15$  km as a function of latitude for NCEP. Equatorward of about  $15^{\circ}$ N/S tropopause height is almost always greater than 15 km, whereas poleward of about  $60^{\circ}$ N/S tropopause height almost never exceeds 15 km with the exception of southern polar latitudes (dotted line in Figure 2; nonzero frequencies there mainly occur during winter where the tropopause is often not well defined). Since latitudes poleward of  $60^{\circ}$  can hardly be considered tropical the frequency of occurrence is set to zero poleward of  $60^{\circ}$ . The dashed line in Figure 2 marks the tropical edge latitudes obtained as described above; that is, the area under the dashed and the solid curves are by definition equal for each hemisphere separately. Frequency of occurrence corresponding to the different frequency thresholds used by SR07 are also shown. Evidently, the tropical edge latitudes as defined here roughly correspond to a frequency of occurrence of 0.5 which is very close to the 200 d/yr frequency threshold.

[21] The above procedure reduces the problem to only one threshold ( $z_{TP}^t$ ). Figure 3 shows the sensitivity of the widening trend to  $z_{TP}^t$  and its corresponding standard error based on  $2\sigma$  uncertainties for each reanalysis data set used in this study. The period 1979–2001 was used for maximum consistency between the different data sets, as constrained by the ERA40 data. Note again that near the subtropical tropopause log-pressure height and geopotential height differ by  $\sim 0.5$  km; that is, using log-pressure tropopause heights instead of geopotential tropopause heights results in a qualitatively similar behavior as shown in Figure 3 with all curves shifted to the left by  $\sim 0.5$  km. In particular, the threshold of 15 km based on log-pressure heights used by SR07 corresponds to a threshold of about 15.5 km based on

geopotential heights used in Figure 3 (indicated by the vertical lines in Figure 3).

[22] As expected based on Figure 1 NCEP exhibits a stable widening trend for  $z_{TP}^t$  roughly within the 14–15 km range. NCEP2 shows very similar behavior (recall that NCEP and NCEP2 use the same underlying model core). However, all other data sets do not exhibit stable trends: widening trends based on NCEP\*, ERA40, and JRA25 all show more or less strong sensitivity to  $z_{TP}^t$ . More importantly, the two data sets with good vertical resolution around the tropopause and a well resolved stratosphere (ERA40 and JRA25) show smaller or insignificant trends than the various NCEP data sets for  $z_{TP}^t$  in the 14–15 km

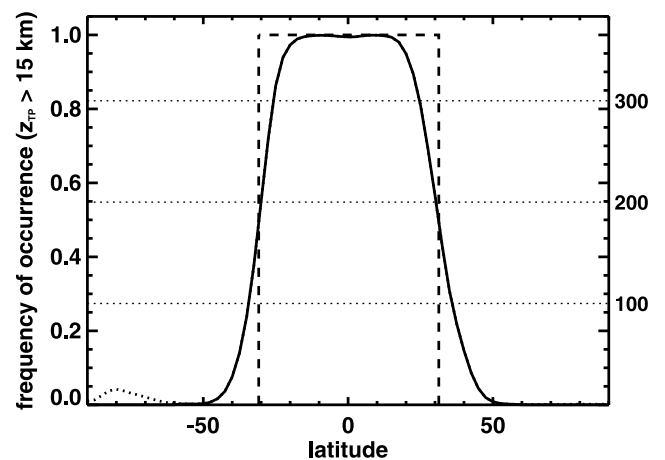


**Figure 2.** Annual mean (1979–2009) frequency of occurrence of tropical tropopause levels (here defined as  $z_{TP} > 15$  km for illustration) as a function of latitude for NCEP. The dashed line marks the area covered by  $z_{TP} > 15$  km for each hemisphere, excluding latitudes poleward of  $60^{\circ}$  (dotted line). Values on the right ordinate and associated thin horizontal dotted lines indicate the number of days per year corresponding to the frequency of occurrence. See text for further details.

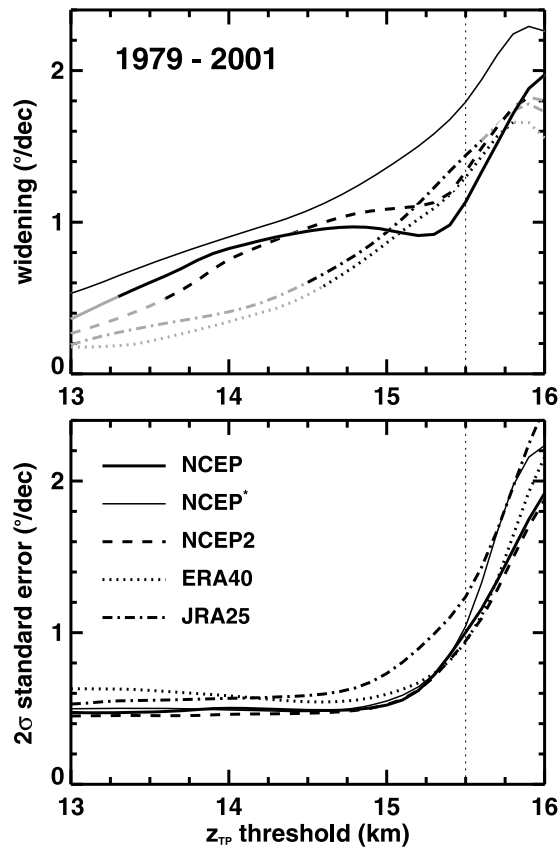


**Figure 3.** (top) Trends in the width of the tropical belt ( $^{\circ}/\text{decade}$ ) for the period 1979–2001 as a function of the tropopause height threshold  $z_{\text{TP}}^t$  (i.e., tropical tropopause levels are defined through  $z_{\text{TP}} > z_{\text{TP}}^t$ ). Nonsignificant trends (based on  $2\sigma$  uncertainties) are indicated in gray. (bottom) Corresponding  $2\sigma$  standard error. The threshold used by SR07 is marked by the vertical dotted lines (converted from log-pressure height into approximate geopotential height). NCEP\* refers to the operational tropopause data provided by NCEP.

range. Interestingly, despite these different sensitivities all widening trends, except for NCEP\*, happen to roughly center around  $1^{\circ}/\text{decade}$  for  $z_{\text{TP}}^t \approx 15$  km, which is consistent with independent estimates in the literature [Seidel *et al.*, 2008; S. M. Davis, personal communication, 2010]. NCEP\* shows the strongest widening trends throughout the range of  $z_{\text{TP}}^t$  values considered. It is also noteworthy that all widening trends shown in Figures 1 and 3 are positive.

[23] Trend uncertainties are generally smaller for the various NCEP data sets than for ERA40 and JRA25 which may reflect missing variability near the tropopause in the NCEP data sets (due to significantly coarser vertical resolution). For all data sets trend uncertainties are roughly constant for values of  $z_{\text{TP}}^t$  below about 15 km, whereas for  $z_{\text{TP}}^t \gtrsim 15$  km the uncertainties strongly increase with increasing  $z_{\text{TP}}^t$ . For example, increasing  $z_{\text{TP}}^t$  by only a small margin from 15 to 15.5 km results in a doubling of the trend uncertainties (at the same time, the widening trends substantially increase for NCEP\*, ERA40, and JRA25 but stay roughly constant for NCEP and NCEP2). In general, as  $z_{\text{TP}}^t$  becomes closer to

typical tropical tropopause heights year-to-year variability in the width estimates (and therefore trend uncertainty) increases.

## 4.2. Objectively Determined Tropopause Height Thresholds

[24] So far, a somewhat arbitrary  $z_{\text{TP}}^t$  value needs to be selected to estimate a widening trend of the tropical belt based on tropopause statistics. In the following, possible ways to define an appropriate  $z_{\text{TP}}^t$  value objectively are investigated. There are at least two reasons to do so. First, as elaborated in section 4.1, widening trends are sensitive to changes in the  $z_{\text{TP}}^t$  value. Second, it is not clear in principle whether  $z_{\text{TP}}^t$  should be constant with time (not even on a seasonal scale) nor whether the same  $z_{\text{TP}}^t$  value should be used for each hemisphere or each data set. It is therefore desirable to define  $z_{\text{TP}}^t$  in a way that allows it to be calculated based on hemispheric tropopause statistics and allows it to be variable in time (e.g., on a seasonal time scale). The latter degree of freedom becomes especially important once century-scale time series are considered on which the tropopause may change considerably [Son *et al.*, 2009; Gettelman *et al.*, 2009] with expected corresponding changes in  $z_{\text{TP}}^t$ .

### 4.2.1. Minimizing Tropical Width Sensitivity to Tropopause Height Threshold

[25] To this end, the sensitivity to changes in  $z_{\text{TP}}^t$  of each hemispheric contribution to the width of the tropics (i.e., not its trend) is considered first (Figure 4). The tropical edge latitudes  $\varphi_{S,N}$  for given  $z_{\text{TP}}^t$ , as defined in section 4.2, serve as an area coordinate based on tropopause height. The southern/northern edge latitude for a given tropopause height threshold  $z_{\text{TP}}^t$  corresponds uniquely to the Southern/Northern Hemispheric area covered by  $z_{\text{TP}} > z_{\text{TP}}^t$ , as well as to the area-weighted hemispheric cumulative frequency at  $z_{\text{TP}}^t$ ,

$$\varphi_{S,N}(z_{\text{TP}}^t) = \arcsin A_{S,N}(z_{\text{TP}} > z_{\text{TP}}^t) = \arcsin(1 - f_c^{S,N}(z_{\text{TP}} = z_{\text{TP}}^t)). \quad (1)$$

Values for  $f_c^{S,N}$  corresponding to  $\varphi_{S,N}$  are indicated in Figure 4 (right-hand vertical axes). The climatological annual mean tropical edge latitudes show a characteristic dependence on  $z_{\text{TP}}^t$  for all data sets considered (Figure 4): they change strongly for  $z_{\text{TP}}^t \gtrsim 15$  km, moderately for  $z_{\text{TP}}^t \lesssim 13$  km, and are least sensitive for  $z_{\text{TP}}^t \sim 14$  km. The strong sensitivity for  $z_{\text{TP}}^t \gtrsim 15$  km, together with larger interannual variability for this  $z_{\text{TP}}^t$  range (Figure 3, bottom), suggest that thresholds above  $\sim 15$  km are not appropriate for estimating tropical width in these data sets. It is important to note that this translates into thresholds above  $\sim 14.5$  km based on log-pressure tropopause heights using a scale height of 7 km. Both the SR07 and Lu *et al.* [2009] results fall into this highly sensitive range. There is very good agreement about the northern edge latitudes from the different reanalyses (they are typically within  $1^{\circ}$  of each other). In the Southern Hemisphere where reanalyses rely more heavily on the underlying model (due to the lack of radiosonde data), estimates of the edge latitudes agree not as well (typically within  $2^{\circ}$  of each other).

[26] With the above described dependency of the tropical edge latitudes on  $z_{\text{TP}}^t$  in mind, the following objective definition for the optimal (“best”) tropopause height threshold (hereafter denoted by  $z_{\text{TP}}^{t_0}$ ) is considered. For any

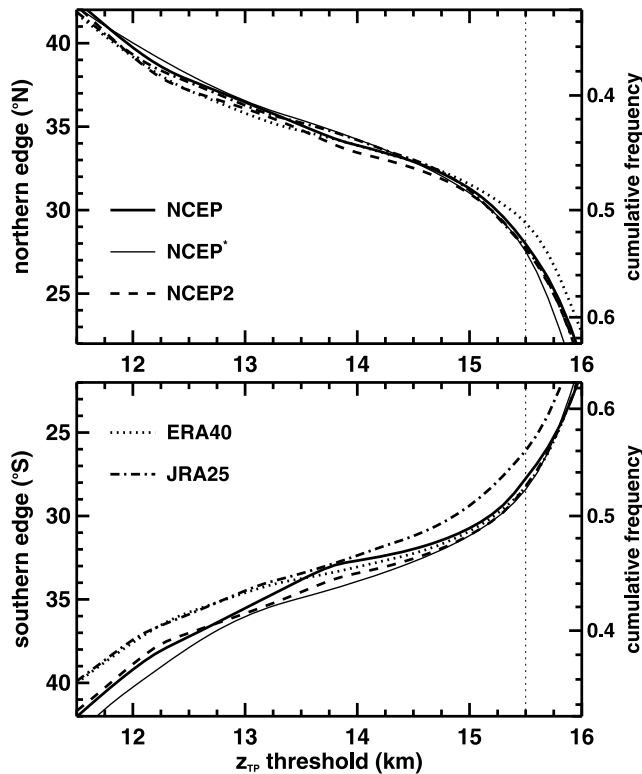


**Figure 4.** Climatological (1979–2001) annual mean tropical edge latitudes  $\varphi_{S,N}$  as a function of the tropopause height threshold  $z_{TP}^t$  for (top) Northern Hemisphere and (bottom) Southern Hemisphere. The threshold used by SR07 is marked by the vertical dotted lines (converted from log-pressure height into approximate geopotential height). The right-hand vertical axes indicate the corresponding area-weighted cumulative frequencies  $f_c^{S,N} = 1 - \sin\varphi_{S,N}$ .

given month and hemisphere,  $z_{TP}^{t,0}$  corresponds to that tropopause height threshold  $z_{TP}^t$  for which the estimated tropical edge latitude  $\varphi_{S,N}$  is least sensitive to changes in  $z_{TP}^t$ . That is, if  $|\partial\varphi_{S,N}/\partial z_{TP}^t|$  describes this sensitivity then  $z_{TP}^{t,0}$  corresponds to the minimum of  $|\partial\varphi_{S,N}/\partial z_{TP}^t|$ . According to the climatology in Figure 4, annual mean values of  $z_{TP}^{t,0} \sim 14$  km are expected (the slope of  $\varphi_{S,N}(z_{TP}^t)$  is shallowest roughly around  $z_{TP}^t \sim 14$  km in Figure 4). Only values for  $z_{TP}^{t,0}$  in the range  $14 \pm 1.5$  km will be considered.

[27] An alternative interpretation of the definition of  $z_{TP}^{t,0}$  is as follows. According to relation (1) we have  $|\partial\varphi_{S,N}/\partial z_{TP}^t| \propto \partial f_c^{S,N}/\partial z_{TP}^t \equiv f_r^{S,N}(z_{TP}^t)$ , where  $f_r^{S,N}(z_{TP}^t)$  is the (area-weighted) hemispheric relative frequency of  $z_{TP}$  at given  $z_{TP}^t$ . The minimum of  $|\partial\varphi_{S,N}/\partial z_{TP}^t|$  (least sensitivity) therefore directly corresponds to a minimum of  $f_r^{S,N}$  (least frequent tropopause height, which is the tropopause height that covers the smallest hemispheric area).

[28] Figure 5 shows hemispheric (area-weighted) climatological annual mean frequency distributions  $f_r^{S,N}(z_{TP})$  for each data set used; that is, Figure 5 corresponds directly to the derivative of the curves shown in Figure 4. As expected, these frequency distributions are predominantly bimodal with a lower broad (extratropical) peak between 8 and 12 km and a higher (tropical) peak between 16 and 17 km.

All data sets show a clear local minimum relative frequency in between these two peaks. As before, less agreement between the relative frequency distributions from different reanalyses is found in the Southern Hemisphere compared to the Northern Hemisphere. A tendency for tropopause heights to cluster around model levels is evident (note the bin size used of 0.1 km is much smaller than the vertical grid spacing of the data sets). In order to obtain robust estimates of the local minimum of  $f_r^{S,N}$ , a filter of 1 km is therefore applied to the individual hemispheric frequency distributions before  $z_{TP}^{t,0}$  is calculated.

[29] The above method to estimate the width of the tropical belt objectively is now used to study the widening of the tropical belt over the period 1979–2009 (1979–2001 for ERA40). Frequency distributions of  $z_{TP}$  for individual months can be somewhat noisy which hampers a robust estimation of  $z_{TP}^{t,0}$  and the resulting edge latitudes on a monthly time scale. Seasonal mean frequency distributions are therefore used. Seasons are defined as January–February–March (JFM), April–May–June (AMJ), etc., mainly for convenience (all data sets used start with January and end with December). The  $z_{TP}^{t,0}$  is obtained separately for each hemisphere and each season based on the smoothed seasonal mean hemispheric relative frequency distributions of  $z_{TP}$ . Tropical edge latitudes are then obtained from the (unfiltered) cumulative frequency corresponding to minimum relative frequency using relation (1) and the width is simply  $\varphi_N - \varphi_S$ .

[30] Both tropical edge latitudes and individual hemispheric tropopause height thresholds undergo strong seasonal cycles (Figure 6). The tropopause height thresholds  $z_{TP}^{t,0}$  generally follow the seasonal cycle of tropical tropopause height [cf. *Seidel et al.*, 2001]: highest during boreal winter/spring and lowest during boreal summer, with peak-to-peak values of around 1 km (somewhat stronger for the Northern Hemisphere). Largest spread amongst the different data sets is found in the Southern Hemisphere during austral summer.

[31] The tropical edge is located closest to the poles during each hemisphere’s summer season and closest to the equator during each hemisphere’s winter season, consistent with the seasonal migration of the subtropical jets. This seasonal cycle has a stronger amplitude in the Northern Hemisphere (peak-to-peak of about  $15^\circ$  latitude) than in the Southern Hemisphere (peak-to-peak less than  $10^\circ$  latitude). The resulting seasonal cycle of the width of the tropical belt shows a semiannual structure (Figure 7) with maxima during the solstice seasons (stronger during boreal summer) and minima during the equinox seasons (stronger during boreal spring). The qualitative structure of this seasonal cycle of the tropical belt width is rather insensitive to changes in the definition of the tropopause height thresholds (not shown).

[32] Figure 8 shows time series for each individual data set of the annual mean width of the tropical belt obtained using the above described seasonally varying tropopause height thresholds  $z_{TP}^{t,0}$ . Both NCEP and NCEP2 data sets show significant positive trends with the stronger trend for NCEP ( $0.7 \pm 0.3^\circ/\text{decade}$ ) and only a marginally significant trend for NCEP2 ( $0.4 \pm 0.4^\circ/\text{decade}$ ). Both of these trend estimates are somewhat smaller but still consistent with other estimates based on different definitions of the tropical belt reported in the literature [*Seidel et al.*, 2008; S. M. Davis, personal communication, 2010]. NCEP\* deviates

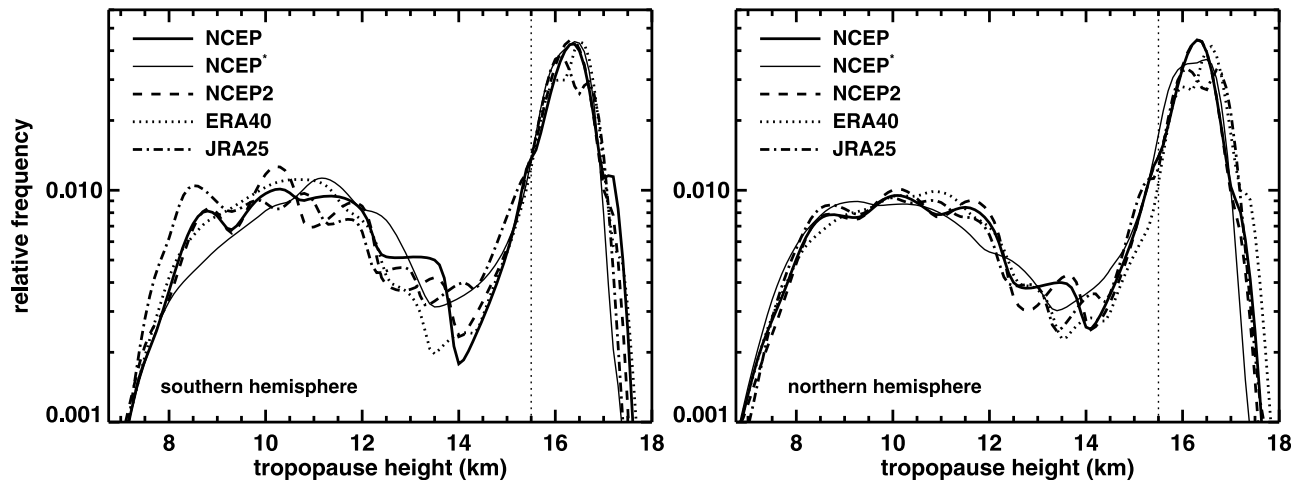


**Figure 5.** Hemispheric mean (area weighted) climatological (1979–2001) annual mean relative frequency distributions of tropopause height for (left) Southern Hemisphere and (right) Northern Hemisphere. Displayed are the unfiltered versions of the frequency distributions obtained with a bin size of 0.1 km. The vertical dotted lines mark the tropopause height threshold used by SR07.

from these two both in terms of the climatological mean value (higher) and the trend (not significant). Despite these differences a striking similarity exists between the interannual variability for all NCEP data sets. The largest width is generally found for the year 1999, the end point of the time

series used by *Lu et al.* [2009]. Pronounced minima in the width of the tropical belt are found following the El Chichon and Pinatubo eruptions in 1982 and 1991, respectively, in agreement with *Lu et al.* [2009]. There is an indication for an overall correlation of the interannual variability of the

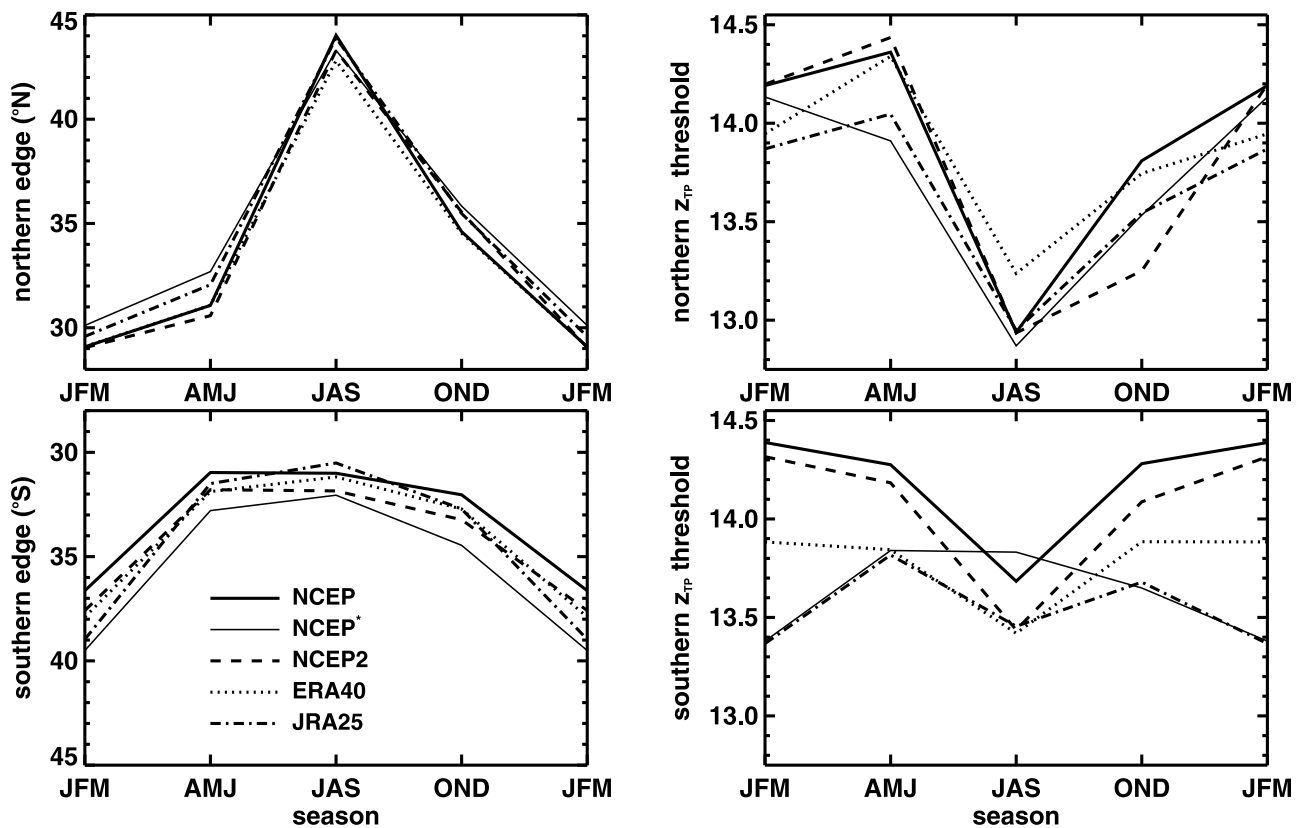


**Figure 6.** Climatological (1979–2001) annual cycle of (left) objectively determined tropical edge latitudes and (right) tropopause height thresholds. (top) Northern Hemisphere. (bottom) Southern Hemisphere. See text for definition of seasons.

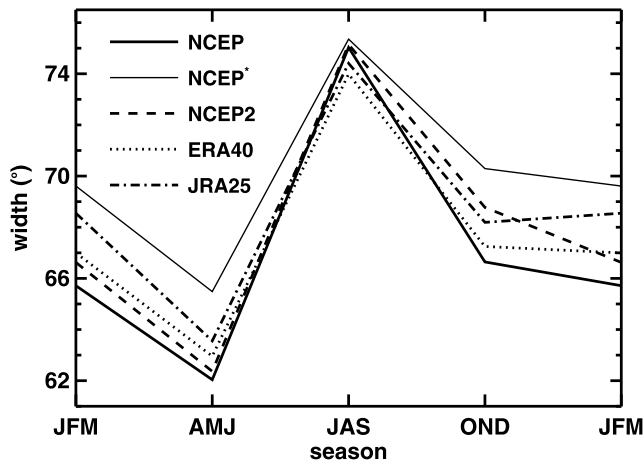


**Figure 7.** Climatological (1979–2001) annual cycle of objectively determined tropical width. See text for definition of seasons.

width of the tropical belt with the El Niño southern oscillation (ENSO): correlation coefficients between annual mean tropical width estimates and the annual mean NINO3.4 index (<http://www.cpc.noaa.gov/data/indices/sstoi.indices>) are  $-0.7$  (NCEP),  $-0.7$  (NCEP\*),  $-0.6$  (NCEP2),  $-0.5$  (ERA40), and  $-0.5$  (JRA25). In particular, the strong peaks in tropical width found in all data sets around 1989 and 2000 correspond to periods of strong La Niña signals. Interestingly, there appears to be somewhat of a downward shift in the time series following the year 2000 (toward smaller widths), comparable in magnitude to the shift following the Pinatubo eruption. To what extent this potential shift is related to the climate shift in tropical tropopause properties as reported by *Randel et al.* [2006] is presently not clear and deserves further study.

[33] The widening trend in ERA40 (only up to 2001) is not significant, whereas the widening trend in JRA25 is

significantly negative ( $-0.5 \pm 0.4^\circ/\text{decade}$ , corresponding to a shrinking of the tropical belt). These two data sets therefore do not confirm the long-term evolution of the width of the tropical belt as obtained from NCEP and NCEP2. Nevertheless, interannual variability is qualitatively similar for all data sets, correlations based on detrended width estimates between ERA40 and the NCEP data sets are in the range 0.5–0.6 and they are in the range 0.6–0.7 between JRA25 and the NCEP data sets.

[34] It is interesting to note that the objectively determined annual mean tropopause height thresholds  $z_{\text{TP}}^{t,0}$  show a positive trend of  $0.07 \pm 0.05$  km for ERA40 and  $0.08 \pm 0.04$  km for JRA25 whereas they remain constant or slightly decrease over the period considered for the NCEP data sets (Figure 9). A temporal minimum in  $z_{\text{TP}}^{t,0}$  exists around the year 2000 which acts to enhance the tropical width maximum in that year compared to a constant tropopause height threshold (see Figure 4, which shows that the width of the tropical belt increases with decreasing  $z_{\text{TP}}^t$ ). Annual mean values for  $z_{\text{TP}}^{t,0}$  generally fall in the range 13.5–14 km with some systematic differences between the different data sets (consistent with Figure 6, right).

[35] Breaking up the width of the tropical belt into the individual hemispheric edge latitudes confirms the above overall picture (Figure 10), but also shows a clear discrepancy between different data sets in the Southern Hemispheric tropical edge. This is somewhat expected given that the Southern Hemisphere is much more data sparse than its northern counterpart; that is, the reanalysis data sets rely more heavily on their underlying model in the Southern Hemisphere (see discussion of Figures 4 and 5). Interestingly, it is the southern tropical edge that causes the overall widening trend of the tropical belt in the case of the NCEP data sets and the shrinking trend in the case of JRA25. Again, there is an apparent change in the trend behavior following the year 2000. Most of the poleward trend in the southern edge latitude comes from the summer season with

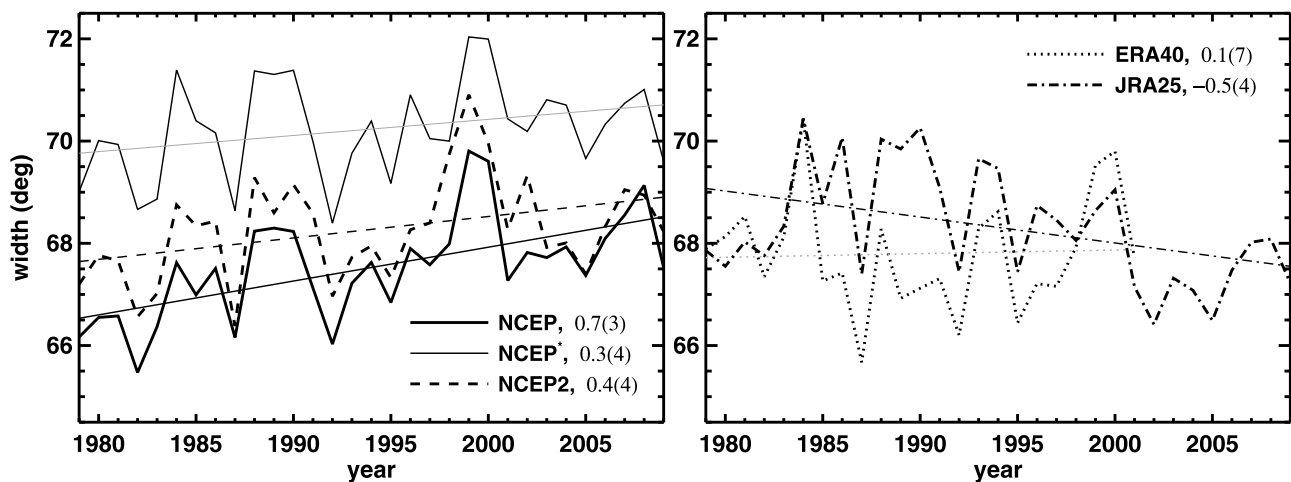


**Figure 8.** Annual mean tropical width for the period 1979–2009 (1979–2001 for ERA40) obtained by objectively determined seasonally varying thresholds in tropopause height (according to the definition in section 4.2.1). Straight lines depict linear trends (nonsignificant trends in gray). Significantly positive trends are only found for the NCEP data sets. Trend values are indicated (in  $^\circ/\text{decade}$ ) for each data set with  $2\sigma$  uncertainties referring to the last digit given in parentheses (e.g., 0.7(3) is to be read  $0.7 \pm 0.3$ ).

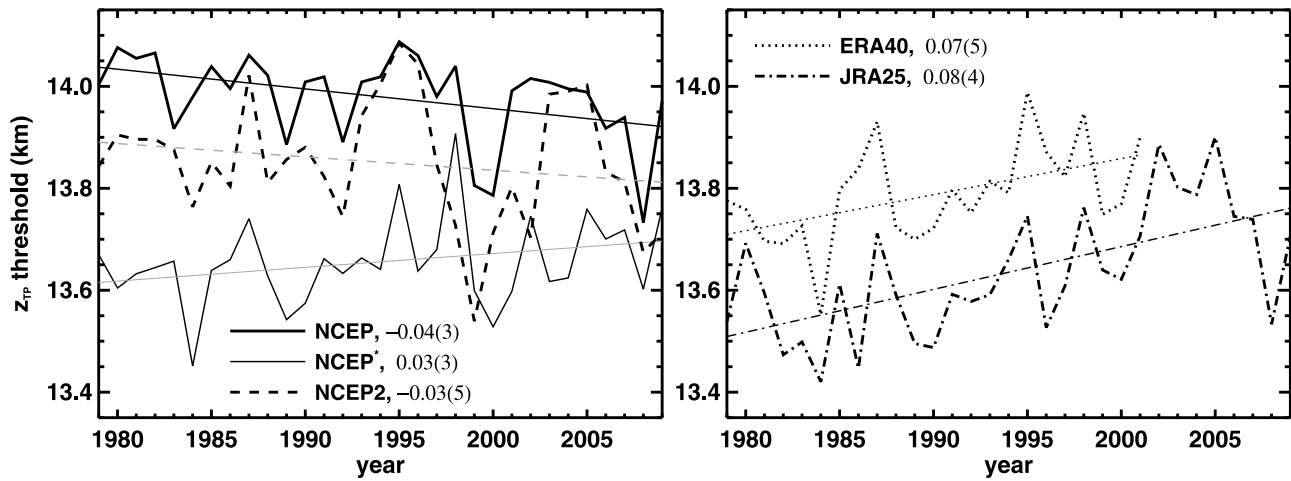


**Figure 9.** Annual mean of objectively determined seasonally varying thresholds in tropopause height (according to the definition in section 4.2.1) for the period 1979–2009 (1979–2001 for ERA40). Straight lines depict linear trends (nonsignificant trends in gray). Trend values are indicated (in km/decade) as in Figure 8.

mostly insignificant trends, even for the NCEP data sets during winter (not shown). SR07 found a strong difference between the two hemispheres in the longitudinal structure to the trend based on the NCEP\* data (see their Figure 6) and this may also contribute to the trend differences between the two hemispheres.

**4.2.2. An Alternative Tropopause Height Threshold Definition**

[36] The definition of the tropopause height threshold corresponding to least tropical width sensitivity presented in section 4.2.1 advantageously provides an objective definition of the edge latitudes of the tropical belt. This property

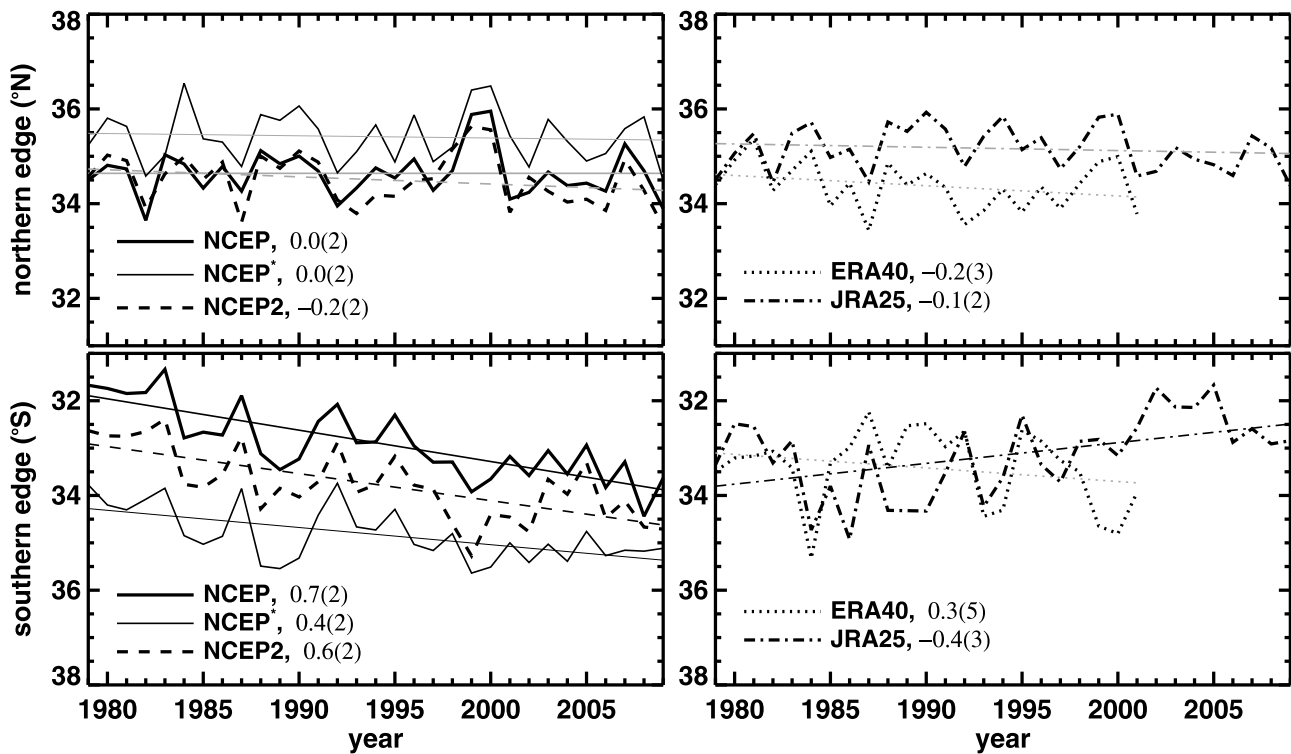


**Figure 10.** Annual mean of objectively determined tropical edge latitudes (according to the definition in section 4.2.1) for the period 1979–2009 (1979–2001 for ERA40) for (top) Northern Hemisphere and (bottom) Southern Hemisphere. Straight lines depict linear trends (nonsignificant trends in gray). Significantly positive trends are only found for the NCEP data sets in the Southern Hemisphere. Trend values are indicated (in °/decade, formatted as in Figure 8).

of objectivity makes this definition of practical use. It is, however, not clear to what extent the condition of least tropical width sensitivity (as associated with the tropopause height that covers the smallest hemispheric area) relates to the tropical edges in a more physical sense. In this regard it is useful to consider the limit of the minimum of the relative frequency  $f_r^{S,N}(z_{\text{TP}})$  going to zero. In this case it would be straightforward to associate the part left of the minimum of the frequency distribution with an extratropical regime and the part right of the minimum of the frequency distribution with a tropical regime. However, the minimum of the actual frequency distributions in Figure 5 does not approach zero, complicating a clear distinction between an extratropical and a tropical regime.

[37] Besides being objective, an advantage of the tropopause height threshold definition presented in section 4.2.1 is that it allows the tropopause height threshold to be a function of time, thereby allowing it to adjust for seasonal, interannual, and long-term changes. An alternative definition that shares this latter property relates the tropopause height threshold to tropopause height statistics of the inner tropics,

$$z_{\text{TP}}^t|_{S,N} \equiv \langle z_{\text{TP}}^r \rangle_{S,N} - d \cdot \sigma_{S,N}^r. \quad (2)$$

Here, the  $\langle z_{\text{TP}}^r \rangle_{S,N}$  denotes the monthly mean tropopause height over the inner tropics (defined by latitudes within  $15^\circ$  of the equator) of a given hemisphere,  $\sigma_{S,N}^r$  denotes the corresponding standard deviation, and  $d$  is a free parameter (restricted to be positive). Annual mean inner tropical tropopause height typically is 16.5 km with a typical standard deviation of about 0.4 km; that is, a factor of  $d \sim 4\text{--}6$  results in annual mean tropopause height thresholds between 14 and 15 km.

[38] Figure 11 shows tropical belt widening trends as a function of the factor  $d$  and their associated  $2\sigma$  standard errors. As in Figure 3, there exists a spread of the trends from different data sets, even though the spread is well within the trend uncertainties. However, in the present case the sensitivity of the widening trends to changes in the free parameter ( $d$ ) are rather small, in particular for values of  $d$  in the range 4–6 (corresponding to annual mean tropopause height thresholds of 14–15 km; see above). Trend uncertainties (related to interannual tropical width variability) are also smallest for  $d$  between 4 and 6 and are not very sensitive to changes in  $d$  in that range. Where significant the trends range from  $0.6^\circ/\text{decade}$  to  $1^\circ/\text{decade}$  for  $d$  between 4 and 6. It is interesting to note that the trends for NCEP2 are exclusively insignificant over the range of  $d$  values considered.

[39] Given the trends are not very sensitive to changes in  $d$  for  $4 \lesssim d \lesssim 6$  one may choose a particular value for  $d$  in that range and evaluate the long-term behavior of the tropical edge latitudes for this particular value. Figure 12 shows the evolution of the annual mean tropopause height threshold for  $d = 5$ . Overall, the resulting values for the tropopause height thresholds range from 14–15 km depending on the data set considered. These values are on the order of 0.5–1 km larger than those obtained from least tropical width sensitivity (see Figure 9). A significant trend is only found for NCEP2 ( $0.07 \pm 0.05$  km/decade) in contrast to the behavior in Figure 9. Nevertheless, interannual

variability is very similar for both ways to obtain a tropopause height threshold. Note that trends in the tropopause height threshold as defined by equation (2) result from a combination of the trends in tropical tropopause height and its standard deviation.

[40] Figure 13 shows annual mean tropical edge latitudes using  $d = 5$  for the period 1979–2009. Significant trends of similar magnitude (around  $0.5^\circ/\text{decade}$ ) are found for the southern edge latitude for all NCEP data sets and ERA40 (only up to 2001). Again, interannual variability is very similar for all data sets with anomalously small tropical widths following the El Chichon and Pinatubo eruptions and anomalously large tropical widths during strong La Niña years (see discussion in section 4.2.1 and Figures 8 and 10). Correlation coefficients between annual mean tropical width estimates and the annual mean NINO3.4 index in this case are  $-0.7$  (NCEP),  $-0.7$  (NCEP\*),  $-0.7$  (NCEP2),  $-0.6$  (ERA40), and  $-0.7$  (JRA25). All northern hemispheric trends are insignificant. Annual cycles of the tropical edge latitudes and tropopause height thresholds are very similar to those shown in Figure 6 (not shown).

[41] The most striking result is therefore that different systematic methods to define the edge of the tropics based on tropopause statistics result in consistent tropical edge estimates with similar seasonal and interannual variability but different long-term trends. In this sense, results presented in this study on the seasonal and interannual variability of the width of the tropical belt seem robust, whereas the trends results seem not robust; depending on the data set and the method used, significantly positive (widening), significantly negative (shrinking), or insignificant (no change) trends are found.

## 5. Summary and Conclusions

[42] The problem of estimating the width of the tropical belt and its corresponding trend over the past three decades from global tropopause statistics based on reanalysis data was revisited. Past studies defined tropical edge latitudes as those latitudes at which the number of days per year with log-pressure tropopause heights above 15 km equals a certain threshold [Seidel and Randel, 2007; Lu et al., 2009]. It was shown that the resulting widening trends based on log-pressure tropopause heights as provided within the NCEP data set (labeled NCEP\*) exhibit large sensitivities to the thresholds used. Slight changes in either one of these thresholds, in particular the tropopause height threshold, result in large changes in the widening trend. Converting the NCEP provided tropopause pressure into tropopause (geopotential) height reduces this sensitivity somewhat. A more accurate determination of tropopause height based on NCEP temperature data on model levels leads to a further reduction of this sensitivity.

[43] In the present study the tropical edge latitudes  $\varphi_{S,N}$  are defined through an area coordinate based on tropopause height statistics: if  $A_{S,N}$  represents the fractional hemispheric area with tropopause heights above a threshold ( $z_{\text{TP}}^t$ ), then  $\varphi_{S,N} = \arcsin A_{S,N}$ . This definition corresponds to an objectively determined frequency threshold in the SR07 definition, which turns out to be very close to 200 d/yr. The resulting trend estimates for the width of the tropics from the various reanalysis data sets still show considerable

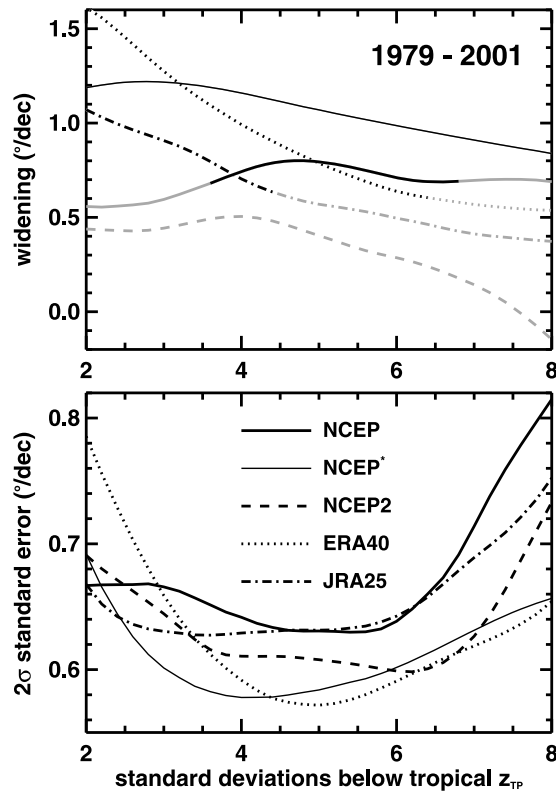


**Figure 11.** (top) Trends in the width of the tropical belt ( $^{\circ}/\text{decade}$ ) for the period 1979–2001 as a function of tropopause height threshold  $z_{TP}^t$  given by the number of standard deviations below the monthly mean tropical tropopause (see equation (2) and section 4.2.2; the abscissa corresponds to  $d$ ). Nonsignificant trends are indicated in gray. (bottom) Corresponding  $2\sigma$  standard error.

sensitivity to the tropopause height threshold, except for NCEP and NCEP2 which show robust trends for  $z_{TP}^t$  within 14–15 km.

[44] An optimal tropopause height threshold ( $z_{TP}^{t,0}$ ) is introduced as corresponding to the minimum of the seasonal

(area-weighted) hemispheric mean relative frequency distribution of tropopause height; that is,  $z_{TP}^{t,0}$  corresponds to that tropopause height which covers the smallest hemispheric area ( $z_{TP}^t$  is the least frequent tropopause height). Defined this way  $z_{TP}^{t,0}$  is a function of time (with temporal resolution of 3 months), hemisphere, and data set. As discussed in section 4.2,  $z_{TP}^{t,0}$  also corresponds to that tropopause height threshold  $z_{TP}^t$  which for a given season and hemisphere shows least sensitivity of the tropical edge latitude to changes in  $z_{TP}^t$ .

[45] A trend analysis based on a time-dependent threshold may appear somewhat inconsistent. However, defining tropical edge latitudes based on global tropopause height statistics requires a clear distinction between tropical and extratropical tropopause heights. The  $z_{TP}^{t,0}$  represents a relative measure quantifying this distinction (as opposed to an absolute measure which would only represent a certain tropopause height, independent of its ability to distinguish tropical and extratropical tropopause heights). Both, tropical and extratropical tropopause heights undergo seasonal, interannual, and long-term changes. The same temporal variability needs to be allowed for in  $z_{TP}^{t,0}$ . Therefore, allowing  $z_{TP}^{t,0}$  to be a function of time seems not just justifiable but in fact desired.

[46] When  $z_{TP}^{t,0}$  is used to define tropical edge latitudes and therefore the width of the tropical belt objectively, only NCEP and NCEP2 exhibit significant widening trends over the period 1979–2009 that are smaller but still consistent with other reported widening trends in the literature [cf. Seidel *et al.*, 2008; S. M. Davis, personal communication, 2010]. ERA40 does not exhibit a significant widening trend (over the period 1979–2001) and JRA25 even exhibits a significant shrinking trend (1979–2009).

[47] An alternative tropopause height threshold definition (see equation (2)) is introduced that is related to monthly tropopause height statistics of the inner tropics. Stable widening trends are found for tropopause height thresholds in the range 4–6 standard deviations below the mean tropical tropopause height. Small but significant widening trends of around  $0.5^{\circ}/\text{decade}$  are found for all NCEP data sets (1979–2009) and ERA40 (1979–2001), but not for JRA25

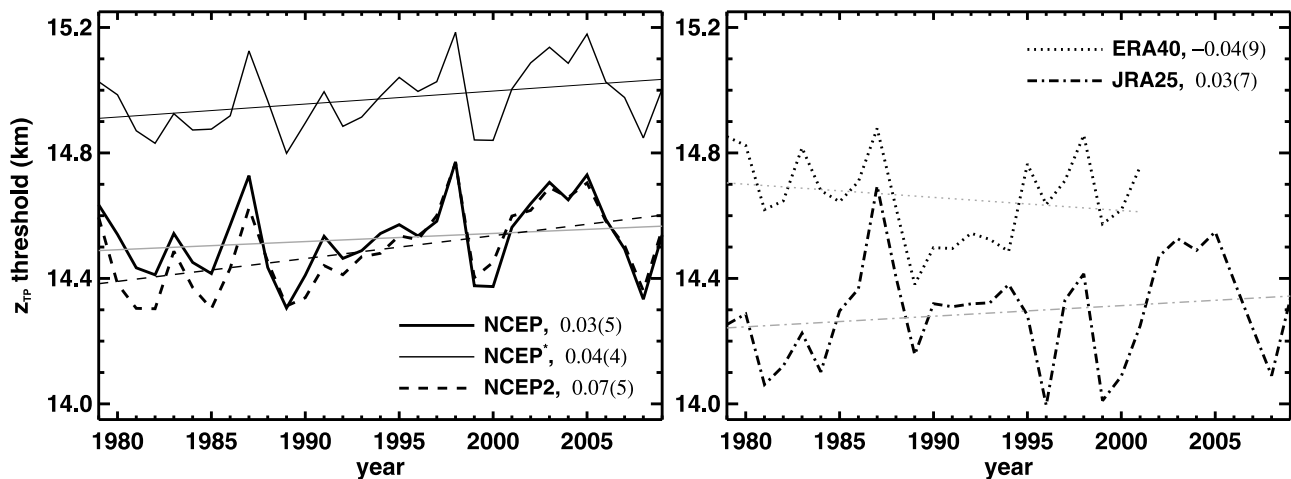


**Figure 12.** Same as Figure 9 but for alternative objective tropopause height threshold definition (see section 4.2.2, equation (2)). A standard deviation factor of  $d = 5$  has been used.

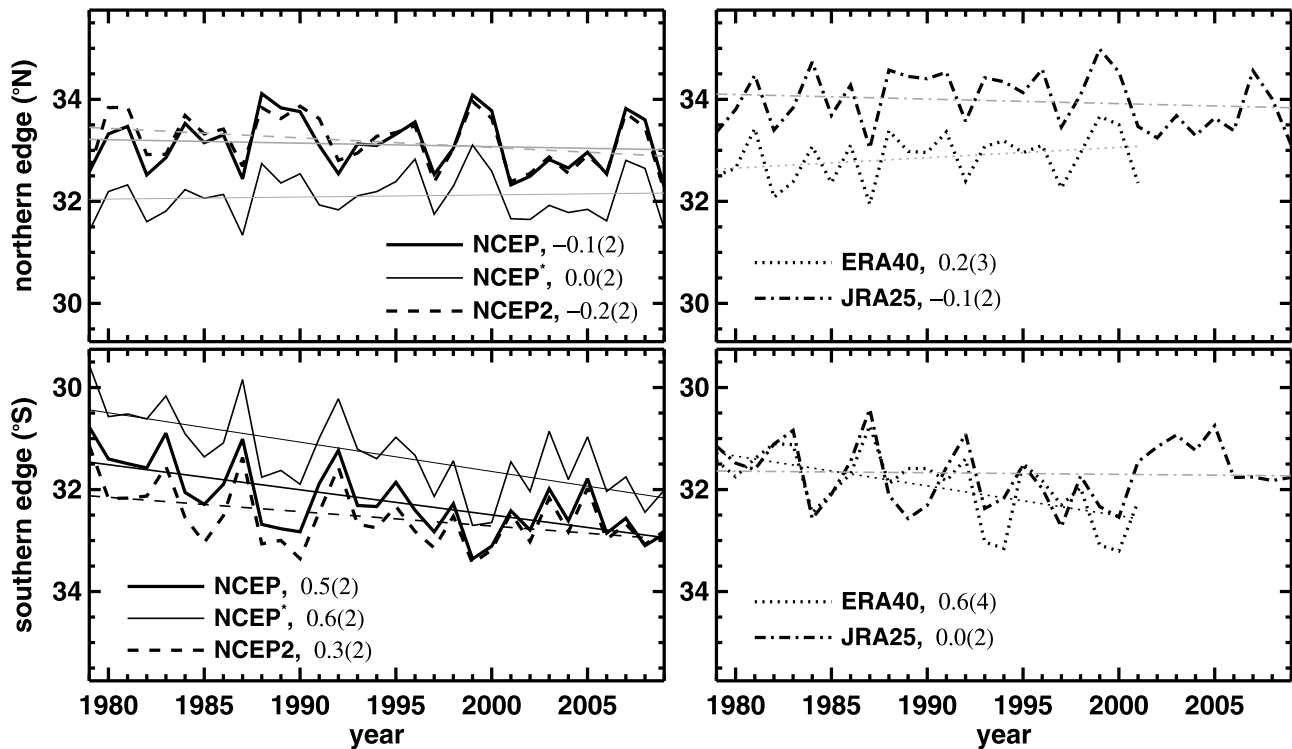


**Figure 13.** Same as Figure 10 but for alternative objective tropopause height threshold definition (see section 4.2.2, equation (2)). A standard deviation factor of  $d = 5$  has been used.

(1979–2009). Nevertheless, seasonal and interannual variability of the tropical edge latitudes is very similar between the different reanalysis data sets and between different tropopause height threshold definitions. It may therefore be concluded that seasonal and interannual variations in tropical edge latitudes based on tropopause statistics from different reanalysis data sets appear robust, whereas the same statement does not hold for long-term trends; neither of the objective methods introduced here produced trends of unanimous sign between the different data sets.

[48] Reanalyses have the advantage over operational analyses that the modeling system is held fixed in time in order to avoid spurious changes in the data due to changes in the modeling system. However, the assimilated data sets exhibit significant changes over time that can lead to inhomogeneities in long-term time series. Due to different data assimilation procedures in different reanalyses these inhomogeneities do not necessarily agree amongst the different data sets. For example, satellite radiances are assimilated directly in the case of the ERA40 and JRA25 data sets, whereas they are converted into temperature before they are assimilated for the NCEP data sets. Furthermore, data assimilation has been shown to act to smooth the vertical temperature structure around the tropopause [Birner et al., 2006].

[49] In closing, it is noted that the separation between the tropical and the extratropical tropopause is strongly influenced by stratospheric dynamics [e.g., Thuburn and Craig, 2000; Birner, 2010]. A relation between certain tropopause properties and the width of the tropical belt (a characteristic of the troposphere) on a physical basis is therefore unclear. With the poor representation of the tropopause region and stratosphere in the NCEP data sets it is conceivable that

the lack of a well-resolved stratosphere leads to an over-emphasized coupling between the tropopause and tropospheric processes in these data sets. As such, certain tropopause properties may somewhat fortuitously serve as an indicator of the width of the tropical belt in the NCEP data sets.

[50] **Acknowledgments.** Useful discussions and comments by Dian Seidel, Bill Randel, Sean Davis, Karen Rosenlof, Kevin Grise, and two anonymous reviewers on an earlier version of the manuscript are gratefully acknowledged. I am especially grateful for the thorough reading of the manuscript and the detailed and constructive reviewer comments by Dian Seidel. Wesley Ebisuzaki kindly provided the computer code for the tropopause algorithm used by NCEP to produce their provided tropopause data. NCEP Reanalysis data were provided by the NOAA/OAR/ESRL PSD, Boulder, Colorado, from their Web site at <http://www.esrl.noaa.gov/psd/>. Access to ERA40 data, originally generated by ECMWF, was provided through the National Center for Atmospheric Research (NCAR). Access to JRA25 data, originally generated by the cooperative research project of the JRA-25 long-term reanalysis by the Japan Meteorological Agency (JMA) and the Central Research Institute of Electric Power Industry (CRIEPI), was also provided through NCAR.

## References

- Añel, J. A., J. C. Antuña, L. de la Torre, J. M. Castanheira, and L. Gimeno (2008), Climatological features of global multiple tropopause events, *J. Geophys. Res.*, *113*, D00B08, doi:10.1029/2007JD009697.
- Birner, T. (2010), Residual circulation and tropopause structure, *J. Atmos. Sci.*, *67*, 2582–2600.
- Birner, T., D. Sankey, and T. G. Shepherd (2006), The tropopause inversion layer in models and analyses, *Geophys. Res. Lett.*, *33*, L14804, doi:10.1029/2006GL026549.
- Butchart, N., and E. E. Remsberg (1985), The area of the stratospheric polar vortex as a diagnostic for tracer transport on an isentropic surface, *J. Atmos. Sci.*, *43*, 1319–1339.
- Frierson, D. M. W., J. Lu, and G. Chen (2007), Width of the Hadley cell in simple and comprehensive general circulation models, *Geophys. Res. Lett.*, *34*, L18804, doi:10.1029/2007GL031115.

- Gottelman, A., et al. (2009), The tropical tropopause layer 1960–2100, *Atmos. Chem. Phys.*, *9*, 1621–1637.
- Hu, Y., and Q. Fu (2007), Observed poleward expansion of the Hadley circulation since 1979, *Atmos. Chem. Phys.*, *7*, 5229–5236.
- Hudson, R. D., M. F. Andrade, M. B. Follette, and A. D. Frolov (2006), The total ozone field separated into meteorological regimes—Part II: Northern Hemisphere mid-latitude total ozone trends, *Atmos. Chem. Phys.*, *6*, 5183–5191.
- Johanson, C. M., and Q. Fu (2009), Hadley cell widening: Model simulations versus observations, *J. Clim.*, *22*, 2713–2725.
- Kalnay, E., et al. (1996), The NCEP/NCAR 40-year reanalysis project, *Bull. Am. Meteorol. Soc.*, *77*, 437–471.
- Kanamitsu, M., W. Ebisuzaki, J. Woollen, S. Yang, J. Hnilo, M. Fiorino, and G. Potter (2002), NCEP–DOE AMIP-II Reanalysis (R-2), *Bull. Am. Meteorol. Soc.*, *83*, 1631–1643.
- Kistler, R., et al. (2001), The NCEP–NCAR 50-year reanalysis: Monthly means CD-ROM and documentation, *Bull. Am. Meteorol. Soc.*, *82*, 247–267.
- Lu, J., G. A. Vecchi, and T. Reichler (2007), Expansion of the Hadley cell under global warming, *Geophys. Res. Lett.*, *34*, L06805, doi:10.1029/2006GL028443.
- Lu, J., C. Deser, and T. Reichler (2009), Cause of the widening of the tropical belt since 1958, *Geophys. Res. Lett.*, *36*, L03803, doi:10.1029/2008GL036076.
- Onogi, K., et al. (2007), The JRA-25 reanalysis, *J. Meteorol. Soc. Jpn.*, *85*, 369–432.
- Randel, W. J., F. Wu, H. Vömel, G. E. Nedoluha, and P. Forster (2006), Decreases in stratospheric water vapor after 2001: Links to changes in the tropical tropopause and Brewer–Dobson circulation, *J. Geophys. Res.*, *111*, D12312, doi:10.1029/2005JD006744.
- Randel, W. J., D. J. Seidel, and L. L. Pan (2007), Observational characteristics of double tropopauses, *J. Geophys. Res.*, *112*, D07309, doi:10.1029/2006JD007904.
- Reichler, T., M. Dameris, and R. Sausen (2003), Determining the tropopause height from gridded data, *Geophys. Res. Lett.*, *30*(20), 2042, doi:10.1029/2003GL018240.
- Seidel, D. J., and W. J. Randel (2007), Recent widening of the tropical belt: Evidence from tropopause observations, *J. Geophys. Res.*, *112*, D20113, doi:10.1029/2007JD008861.
- Seidel, D. J., R. J. Ross, J. K. Angell, and G. C. Reid (2001), Climatological characteristics of the tropical tropopause as revealed by radiosondes, *J. Geophys. Res.*, *106*, 7857–7878.
- Seidel, D. J., Q. Fu, W. J. Randel, and T. J. Reichler (2008), Widening of the tropical belt in a changing climate, *Nat. Geosci.*, *1*, 21–24.
- Son, S.-W., L. M. Polvani, D. W. Waugh, T. Birner, H. Akiyoshi, R. R. Garcia, A. Guttman, D. A. Plummer, and E. Rozanov (2009), The impact of stratospheric ozone recovery on tropopause height trends, *J. Clim.*, *22*, 429–445, doi:10.1175/2008JCLI2215.1.
- Thuburn, J., and G. C. Craig (2000), Stratospheric influence on tropopause height: The radiative constraint, *J. Atmos. Sci.*, *57*, 17–28.
- Uppala, S. M., et al. (2005), The ERA-40 re-analysis, *Q. J. R. Meteorol. Soc.*, *131*, 2961–3012.
- World Meteorological Organization (1957), Meteorology—A three-dimensional science, *WMO Bull.*, *6*, 134–138.

---

T. Birner, Department of Atmospheric Science, Colorado State University, 1371 Campus Delivery, Fort Collins, CO 80523-1371, USA. (thomas@atmos.colostate.edu)